Coherent Optical-Fiber Link Across Italy and France

Coherent Optical-Fiber Link Across Italy and France

C. Clivati,[1] M. Pizzocaro,[1,*] E.K. Bertacco,[1] S. Condio,[1,†] G.A. Costanzo,[1,†] S. Donadello,[1] I. Goti,[1,†] M. Gozzelino,[1] F. Levi,[1] A. Mura,[1] M. Risaro,[1] D. Calonico,[1] M. Tønnes,[2] B. Pointard,[2] M. Mazouth-Laurol,[2] R. Le Targat,[2] M. Abgrall,[2] M. Lours,[2] H. Le Goff,[2] L. Lorini,[2] P.-E. Pottie,[2] E. Cantin,[3] O. Lopez,[3] C. Chardonnet,[3] and A. Amy-Klein[3]

[1] *Istituto Nazionale di Ricerca Metrologica (INRIM), Strada delle cacce 91, Torino 10135, Italy*
[2] *LNE-SYRTE, Observatoire de Paris—Université PSL, CNRS, Sorbonne Université Paris, France*
[3] *Laboratoire de Physique des Lasers (LPL), Université Sorbonne Paris Nord, CNRS, Villetaneuse, France*

(Received 21 June 2022; accepted 13 September 2022; published 3 November 2022)

The dissemination of atomic clocks with fiber-based techniques finds application in the fields of metrology, fundamental physics, navigation, and spectroscopy but is a challenge in terms of reliability, maintenance, and performance. Here, we describe the realization of a 1023-km-long fiber link between the metrological institutes of Italy and France that shares the infrastructure with the Internet traffic and exploits segmentation in shorter, cascaded spans to fight optical losses exceeding 280 dB. With four months of quasicontinuous operation of this link, we compared the Cs, Rb, and Yb atomic clocks at our laboratories, highlighting the potential of this tool to assess the clock uncertainty budgets, characterize advanced satellite techniques, and develop optical timescales. The integration of the metrological, fiber-based infrastructures in the two countries, connecting photonics and spectroscopy laboratories as well as telescope facilities, provides the research community with a physical layer over which applications can be built on.

DOI: 10.1103/PhysRevApplied.18.054009

I. INTRODUCTION

Precision spectroscopy of atoms or ions is an important resource for timekeeping, navigation, and fundamental science. The second, unit of time in the International System, is defined upon the ground-state hyperfine transition of the ^{133}Cs atom, and its best realizations achieve an uncertainty in the low 10^{-16} [1–11]. For a few years now, atomic clocks based on optical transitions of neutral atoms or ions demonstrated an even lower uncertainty in the 10^{-18} range [12–15]. The comparison of different atomic clocks led to the recommendation of secondary representations of the second, in view of a future redefinition on a single or a set of optical transitions [16–18]. Before this redefinition becomes possible, independent interlaboratory comparisons of optical clocks both against other optical and primary clocks must be demonstrated. Interspecies atomic clock comparisons, particularly those involving microwave and optical transitions, are also at the heart of physics measurements that constrain the possible variations of fundamental constants [19,20].

In this frame, a network comprising clocks developed by different teams at different institutions leverages the scientific opportunities beyond those of the single laboratory [21,22], but until recently, the instability of satellite-based time-and-frequency transfer techniques was a significant limitation. For instance, the Bureau International des Poids et Mesures (BIPM) maintains the coordinated universal time (UTC), which is the current standard for global timekeeping, from data including both primary and secondary frequency standards and satellite comparisons [23]. Atomic clocks contributing to UTC are routinely compared using the data that appear in the BIPM Circular T bulletin. However, only a few bilateral fountain [24] and optical clock [25–29] comparisons have been performed. The coherent transfer of optical signals across phase-stabilized fibers [30–37], now covering distances of up to thousands of kilometers, represented a breakthrough in this respect, enabling clock comparisons where the space separation no longer contributes to the final uncertainty [5,12,32,38–40].

In this work, we present the permanent 1023-km phase-stabilized fiber link that connects the French and Italian National Metrology Institutes LNE-SYRTE in Paris and INRIM in Torino. We report on the comparisons between three species of atomic clocks among those available at the

*m.pizzocaro@inrim.it
†Also with Politecnico di Torino, corso Duca degli Abruzzi 24, 10124 Torino, Italy.

two institutes, namely two Cs fountain clocks [8,10], a Rb fountain clock [9,10], and an optical Yb lattice clock [41]. Our clock comparison covered four months, demonstrating the degree of maturity achieved by long-haul optical-fiber links in terms of maintenance and uptime. This link is among the few examples of thousand-kilometer-scale optical connections [32–35] and is intended as a tool for scientific tasks that require the regular and long-term comparison of atomic clocks, among which are the periodical assessment of frequency standards, the validation of advanced satellite techniques [28,42,43], the generation of optical timescales [44–48], and tests of relativity [22].

This paper is organized as follows. Section II presents the description of the optical link and its characterization. Section III discusses the result of the clock comparison between the two Cs fountain clocks, the Rb fountain clock, and the optical Yb lattice clock. A conclusion is given in Sec. IV.

II. THE OPTICAL LINK

A. Setup description

The present link connects the Italian Quantum Backbone (IQB) [34] and the French National Research Infrastructure REFIMEVE [49,50], both of which provide frequency references to scientific users in the two countries, serving high-precision atomic and molecular spectroscopy, quantum physics and photonics laboratories [51–54], radio telescopes [25,55], and the national space agencies campuses [34]. Time and rf-frequency transfer to companies and satellite navigation facilities is also being developed, using the White Rabbit technique [56,57]. In addition, via the REFIMEVE network, cross-border connections to the National Metrology Institutes of Germany (PTB) and UK (NPL) are possible [35]. A sketch of the Paris to Torino network is shown in Fig. 1(a). It is composed of a 1023-km cascaded link, in which the optical length of the fibers is actively stabilized using the Doppler noise cancelation technique [58]. An ultrastable radiation at 1542.14 nm is generated at SYRTE by frequency locking a diode laser to a high-finesse optical cavity. Its frequency is constantly measured and steered to a local H maser by an optical frequency comb, thus providing a connection to the local frequency standards. This optical signal is distributed via a stabilized fiber to INRIM, where it is frequency measured against the local H maser using another optical comb.

The link is established using installed telecom fibers provided by the French academic network RENATER and the regional network AMPLIVIA on the French side, and by Consortium TOPIX on the Italian side. These fibers implement dense- and coarse-wavelength-division multiplexing, where channel 44 of the International Telecommunication Union grid, corresponding to a central wavelength of 1542.14 nm, is reserved for frequency dissemination, and the others are used for data traffic. The coherent radiation is periodically extracted from the shared fiber to bypass the standard network equipment that does not sustain the bidirectional operation required for the Doppler noise cancelation, and then injected back. The link is split into six segments with intermediate terminals located in Paris (datacenter TH2), Lyon, Grenoble, Modane, and Frejus tunnel (across the Alps on the Italy-France border) and lengths of 11, 597, 118, 143, 7, and 147 km respectively. Each terminal hosts a repeater laser station (RLS) or a multibranch laser station (MLS), where the metrological signal is regenerated by phase locking a diode laser to the incoming radiation, and phase stabilization of the subsequent segments is performed. MLSs implement star connections that allow the simultaneous stabilization of links to multiple terminals [59]. RLSs and MLSs are engineered in such a way that the transmitted signal is independent of the local rf oscillator, relaxing the need for an accurate and stable rf reference. In addition, 11 bidirectional erbium-doped fiber amplifiers are utilized to partly recover from the signal attenuation on more lossy segments. The segmentation approach, described in detail in Refs. [30,34,37,49,59], is necessary to support the link operation, as the overall one-way power loss exceeding 280 dB could not be compensated using fiber amplifiers only. It also improves the link phase noise suppression by reducing the radiation round-trip delay as compared to a nonsegmented link. The amplifiers and intermediate terminals are operated remotely.

B. Characterization

The noise affecting the distributed frequency signal results from a partially unsuppressed fiber noise, whose cancelation is limited by the link delay that reduces the control bandwidth [58], as well as temporary loss of coherence due to failures of the stabilization electronics (cycle slips), and other uncontrolled effects causing long-term instability or a potential deviation from the nominal frequency. While the instability due to the delay-unsuppressed noise averages down as the inverse of the measurement time, the other effects result in significant frequency bias if affected points are included in the measurement. Synchronously to the link operation it is hence important to validate its performances, detect and remove invalid points. To this end, we established independent phase-stabilized links using the second fiber of the pair, which is always provided by the network operators. By phase comparing the disseminated light on a suitable combination of the two links, it is possible to derive an upper limit for the frequency dissemination uncertainty contributed by each one. In detail, we adopted the scheme shown in Fig. 1(b) to separately characterize the segments SYRTE-TH2, TH2-Modane, and Modane-INRIM.

The SYRTE-Modane link is built by delivering the ultrastable radiation from SYRTE to TH2, where a MLS

FIG. 1. Geographical layout of the infrastructure, with the link between SYRTE, Paris (France) and INRIM, Torino (Italy) characterized in this work highlighted as a thick line. The map also shows the other branches of the REFIMEVE network in blue and the Italian Quantum Backbone (IQB) in red. Cross-border connections of this infrastructure to the National Metrology Institutes NPL in the UK and PTB in Germany are indicated in orange and green. Repeater laser stations (RLS or MLS) and link terminals are represented with open circles. (b) The scheme used for the link characterization: blue paths indicate phase-stabilized links on the two fibers. At SYRTE, local reference light is sent to a photodiode together with the light disseminated through the loop SYRTE-TH2-SYRTE and phase compared to a local rf reference, to evaluate the overall uncertainty of the SYRTE-TH2-SYRTE link (similarly for the path to Modane). The green arrow represents a free-running link whose noise is removed offline. This is detected by heterodyning local radiation at INRIM with light traveling the path INRIM-Modane-INRIM (orange line). The Modane-INRIM link is evaluated by comparing light disseminated through the two fibers.

distributes it further to Modane through cascaded RLSs located in Lyon and Grenoble. A part of the regenerated signal in TH2 is instead sent back to SYRTE using the second fiber of the pair, independently stabilized in the MLS, and here compared to the reference input light (actively stabilized paths are indicated by blue arrows in the figure). This provides a measurement of the frequency distributed along the whole SYRTE-TH2-SYRTE loop, and allows deriving an upper limit to the SYRTE-TH2 dissemination uncertainty. Similarly, from TH2, the regenerated light is sent to Modane via phase-stabilized fiber segments also including intermediate RLSs in Lyon and Grenoble. In Modane, the radiation is regenerated, partly sent back to TH2 using the second fiber, and there compared to the

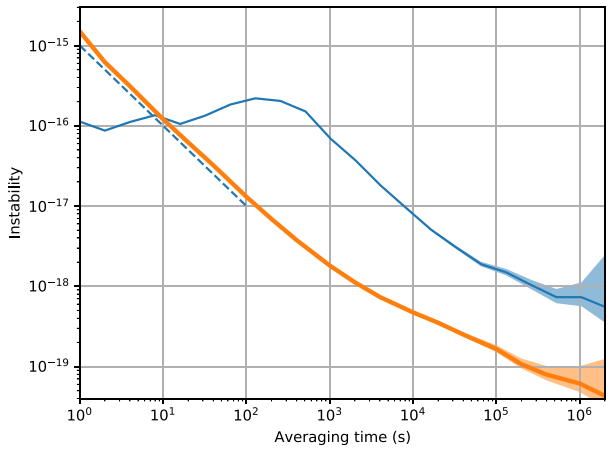

FIG. 2. Measured and expected instability of the link: the orange continuous line corresponds to the end-to-end link instability of the SYRTE-Modane-SYRTE link; the blue solid line shows the measured instability of the INRIM-Modane segment, dominated by that of the validation link (see the text); these instabilities are calculated from four months of data as overlapping Allan deviation and shaded regions denote the uncertainty; the blue dashed line represents the expected instability of the Modane-INRIM link from delay-unsuppressed noise.

reference light to characterize the TH2-Modane segment. The resulting end-to-end instabilities of the SYRTE-TH2-SYRTE and TH2-Modane-TH2 links are quadratically summed to derive the overall instability of the SYRTE-Modane-SYRTE link, as shown in Fig. 2 (orange line). In the short term, it is limited by the delay-unsuppressed noise of the forward and return links. Short optical paths whose length cannot be fully stabilized, mainly contained in the TH2 multibranch station [59], contribute an additional instability that emerges at averaging times of a few thousand seconds and is at the level of 1×10^{-19}. No deviation from the nominal frequency is observed at this level, and we assume this value as the ultimate uncertainty contribution for the SYRTE-Modane segment.

The characterization of the Modane-INRIM segment follows a different scheme, as it is not possible to install any counting equipment in Modane. In Modane, the local regenerated light is split into two parallel links to INRIM, one of them being actively noise canceled to disseminate the signal to INRIM, the second one being used for the uncertainty and instability assessment. The first exploits two RLSs in Modane and the Frejus tunnel [actively stabilized paths are indicated by blue arrows in Fig. 1(b)]. At INRIM the incoming radiation is regenerated and distributed locally. The noise of the second link [green arrow in Fig. 1(b)] is instead continuously recorded and removed offline [60,61]. This is achieved by sending local ultrastable radiation from INRIM to Modane and back, comparing it with the reference light at INRIM [orange arrow in Fig. 1(b)]. The residual noise of the Modane-INRIM segment is then computed by comparing the light distributed through the two independent links.

The instability of the processed signal is shown in Fig. 2 (blue line). Unlike the end-to-end characterization, this scheme partly rejects the delay-unsuppressed noise because the two links are established between the same starting and ending points and because the two fibers are housed in the same cable, so their noise is mostly correlated [62,63]. The short-term instability is thus lower than the instability expected for this link from delay-unsuppressed noise (dashed line in Fig. 2) [64]. For integration times longer than 10 s, the measured instability is higher than the SYRTE-Modane segment and the delay-unsuppressed noise contribution for this span. This is due to about 3 m of uncompensated fibers exposed to temperature variations in Modane, which could not be avoided due to space constraints at this terminal. This contribution will be reduced in the future by modifying the interferometer design inside the RLS in Modane. Uncompensated fibers are present only on the link used for validation and not on the one used for the actual dissemination: we thus expect the dissemination link to exhibit a lower instability, comparable to that observed on the SYRTE-Modane span. Overall, this configuration enables us to spot long-term effects, frequency bias, and cycle slips both in the optical phase-locked loops and in the noise-cancelation loops. Even considering the reported results as an upper limit to the dissemination on the Modane-INRIM segment, the instability reaches 6×10^{-19} and no deviation from the nominal frequency is observed at this level. We assume this value as the ultimate uncertainty for this link. The uncertainty of the optical link between SYRTE and INRIM is thus $< 1 \times 10^{-18}$, which is suitable for the comparison of state-of-the-art optical clocks.

This setup has been operated almost continuously for four months. To ensure a high level of uptime and autonomous operation, all terminals are equipped with automated control of the polarization of incoming radiation, relock algorithms to recover from failures, and operator alert systems. Figure 3 shows the link uptime as a function of the modified Julian date (MJD), calculated daily, over the period from MJD 59514 (October 27, 2021) to MJD 59634 (February 24, 2022). The figure shows the uptime of each stage, including the transfer laser frequency measurements at the two combs and local distribution links between laboratories at SYRTE and INRIM. Downtimes are mostly due to unlocks caused by nonstationary events on the long deployed fiber, such as fast polarization changes or human interventions along the link, or temporary interruptions of end-to-end measurements. The combined uptime of the full chain, shown in the lowermost panel, is 57% on average over the full period, including winter holidays, and reaches 72% on the month between MJD 59583 and 59614 (January

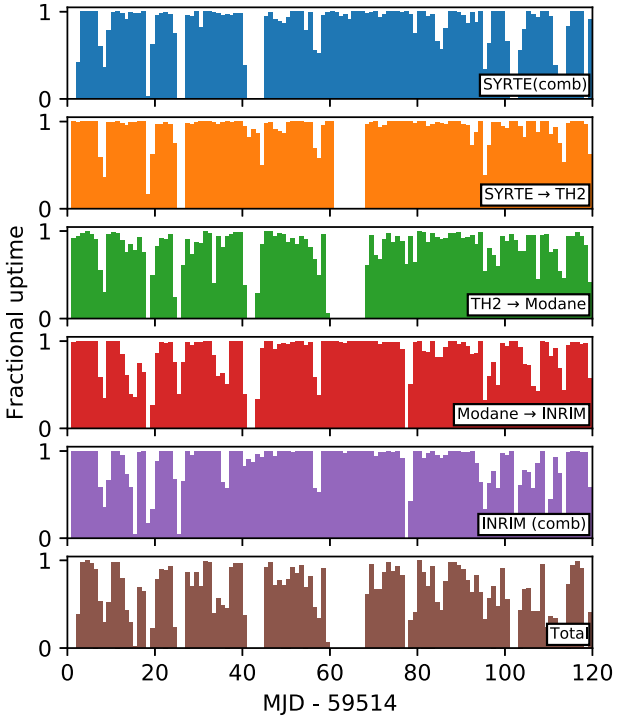

FIG. 3. The daily uptime of individual segments and the combined uptime of the whole link over the four months from October 27, 2021 to February 24, 2022.

4 to February 4, 2022), highlighting the remarkable level of reliability achieved for this infrastructure, also thanks to the automated supervision of the fiber network and terminals.

III. CLOCK COMPARISONS

A. Cs and Rb fountain clocks

As an application, we performed a comparison of the microwave fountain clocks SYRTE FO2 and INRIM IT-CsF2. SYRTE FO2 is a dual fountain that operates with Cs and Rb atoms simultaneously [9,10]. The two parts of FO2, named FO2-Cs and FO2-Rb, are independent frequency standards: FO2-Cs is a primary frequency standard and FO2-Rb, based on the hyperfine transition of ^{87}Rb, is a secondary representation of the second [18,65]. The systematic uncertainty of these two fountains is between 2×10^{-16} and 3×10^{-16}. Their local oscillator is a cryogenic sapphire oscillator, phase locked to a H maser: it grants a stability of $3.2\times10^{-14}/\sqrt{\tau/\mathrm{s}}$ for FO2-Cs and $2.9\times10^{-14}/\sqrt{\tau/\mathrm{s}}$ for FO2-Rb, τ being the measurement time, in full density mode. The density shift is evaluated in real time by alternating full and half density modes: with this measurement protocol, most of the uncertainty due to zero-density extrapolation averages down as $\sqrt{\tau}$ and contributes to the statistical uncertainty [66]. After density correction, systematic uncertainty becomes dominant after 3–4 d.

IT-CsF2 is the Italian primary frequency standard [8]. It is a cryogenic Cs fountain clock with a 2×10^{-16} stated uncertainty. The local oscillator for this clock is a BVA quartz phase locked to a H maser, contributing a short-term instability of $2\times10^{-13}/\sqrt{\tau/\mathrm{s}}$.

Typically, a measurement time of one month is necessary to reduce the statistical uncertainty of IT-CsF2 below the level of systematic. Here we extended the comparison to four months, since all the blocks of the measurement chain can be operated with only minor human intervention. The data processing was performed in two steps. In the first step, following the procedure explained in Ref. [67], the frequency ratio between the two remote H masers was obtained by combining the transfer oscillator frequency measurements on the two remote combs with the link data, excluding points where any of the measurements showed anomalous values or cycle slips. To this end, acquisitions at the counting terminals (SYRTE, TH2, and INRIM) were synchronized to better than 1 s. The synchronization signal was based on local realizations of UTC [UTC(IT) and UTC(OP) at INRIM and SYRTE], while in TH2 it was delivered via a White Rabbit link [56]. In the second step, validated data were averaged in bins with nominal duration of 864 s. Only bins with more than 50% valid data were considered. Fountain data, representing measurements of the H masers with the local microwave clocks, were sampled to the same 864-s grid and combined with the former. Data were processed as fractional frequency ratios $y = r/r_0 - 1$, where r is the physical frequency ratio (or absolute frequency) and r_0 is an arbitrary reference ratio (or reference absolute frequency). This is a common technique to avoid computational problems with numbers with many digits and to linearize equations [67].

Figure 4(a) shows the fractional frequency deviations of FO2-Cs/IT-CsF2 and FO2-Rb/IT-CsF2 obtained via the link, as well as the local measurement FO2-Rb/FO2-Cs at SYRTE, averaged over 864 s. For Rb, we chose the reference frequency to be consistent with the secondary representation of the second for the Rb transition of 6 834 682 610.904 312 6 Hz, which has an uncertainty of 3.4×10^{-16}, as established by the Consultative Committee for Time and Frequency, CCTF, in 2021 [65]. Figure 4(b) shows in full-color symbols the same data averaged in the periods corresponding to the Circular T bulletins n. 407 to n. 410 (from November 2021 to February 2022) [68]. The averages are for 30, 35, 30, and 25 d respectively. The shaded areas represent the $\pm1\sigma$ confidence region for the average fractional frequency ratios over the entire campaign. Open symbols represent the remote comparisons FO2-Cs/IT-CsF2 and FO2-Rb/IT-CsF2 obtained from data that appeared in the Circular T bulletins, which are consistent but have a larger uncertainty coming from the satellite comparison as calculated by the BIPM. All uncertainties

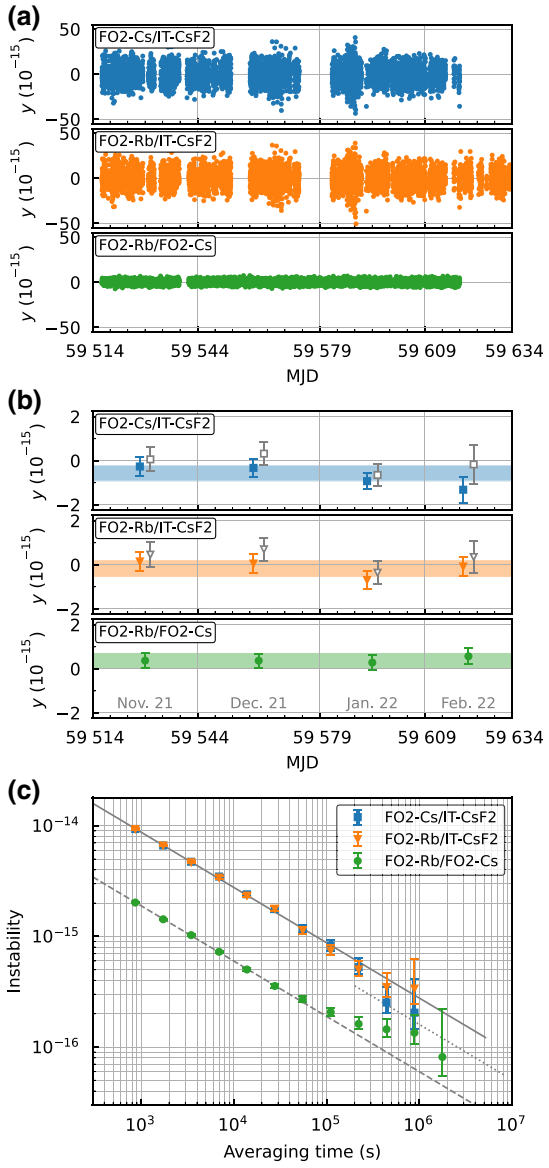

FIG. 4. (a) The fractional frequency ratios FO2-Cs/IT-CsF2, FO2-Rb/IT-CsF2 obtained via the link, as well as the local FO2-Rb/FO2-Cs at SYRTE as a function of the modified Julian date (MJD); each point represents an average over 864 s. (b) Colored points represent the average of the remote and local ratios in the periods of four Circular T bulletins (30, 35, 30, and 25 d, respectively); the colored shaded regions represent the averages over the entire campaign; open gray points show the remote ratios as deduced from data in the Circular T bulletins. All uncertainties correspond to $\pm 1\sigma$ and include the systematic uncertainty of the fountains. (c) Corresponding instabilities of the three ratios as overlapping Allan deviations; the solid gray line represents the white noise contribution of IT-CsF2 (2.8×10^{-13} at 1 s); the dashed gray line represents the short term combined white noise contribution of FO2-Rb/FO2-Cs (6×10^{-14} at 1 s). For FO2-Rb and FO2-Cs, the contribution due to zero-density extrapolation shows up in the Allan deviation for averaging times longer than the period used to calculate the density shift (gray dotted line) and is expected to be $1.6 \times 10^{-13}/\sqrt{\tau/\mathrm{s}}$ from historical data.

include the systematic uncertainties of the fountains. The instabilities of the fiber comparisons are shown in Fig. 4(c) as overlapping Allan deviations. The remote comparison is limited by the instability of IT-CsF2 ($2.3 \times 10^{-13}/\sqrt{\tau/\mathrm{s}}$). The instability of the local comparison at SYRTE is $6 \times 10^{-14}/\sqrt{\tau/\mathrm{s}}$ in the short term. For averaging times $\tau >$ 1 d, the instability is expected to be $1.6 \times 10^{-13}/\sqrt{\tau/\mathrm{s}}$ because of the protocol used to extrapolate data at zero density, as calculated from historical data (ten-years-long dataset). The comparison results are summarized in Table I. The average frequency deviation between FO2-Cs and IT-CsF2 is $y(\text{FO2-Cs/IT-CsF2}) = -5.5(3.7) \times 10^{-16}$. Here the statistical uncertainty is 1.3×10^{-16} with 56.1 d of measurement time derived from the instabilities shown in Fig. 4(c). The result for FO2-Rb/IT-CsF2 is $y(\text{FO2-Rb/IT-CsF2}) = -1.5(3.8) \times 10^{-16}$ where the statistical uncertainty is 1.3×10^{-16} with 60.1 d of measurement time. This corresponds to an absolute frequency of Rb of 6 834 682 610.904 311 4(26) Hz. In these comparisons, the uncertainty of the link contributes negligibly with an uncertainty lower than 6×10^{-19}. The local comparison at SYRTE FO2-Rb/FO2-Cs in the same period results in an average of $y(\text{FO2-Rb/FO2-Cs}) = 3.7(3.5) \times 10^{-16}$, which corresponds to an absolute frequency of Rb of 6 834 682 610.904 315 1(24) Hz. The interlaboratory comparison confirms and validates the stated uncertainties of the clocks.

B. Measurements with IT-Yb1

During the campaign, INRIM operated the optical clock IT-Yb1 [41,69] for 7 d from MJD 59563 to 59570 (December 15–21, 2021). IT-Yb1 is a neutral-Yb lattice clock with instability of $2 \times 10^{-15}/\sqrt{\tau/\mathrm{s}}$ and uncertainty 2.1×10^{-17}. For this measurement, the 1156.84-nm ultrastable laser, subharmonic of the 578.42-nm clock-transition wavelength, was sent to the optical comb at INRIM and compared to the 1542.14-nm laser signal received from the fiber link, using the comb as a transfer oscillator [70]. The comb contribution to the measurement uncertainty was brought to $<1\times10^{-18}$ by operating in a single branch configuration, where both the 1156- and 1542.14-nm laser beams were compared to the same, broadband comb output spanning the full 1- to 2-μm spectrum. The analysis followed the same procedure as in Sec. III A. Figure 5 shows the measured instability for the two remote ratios IT-Yb1/FO2-Cs and IT-Yb1/FO2-Rb and the local ratio IT-Yb1/IT-CsF2. The instabilities are dominated by the contribution of the fountains: $4 \times 10^{-14}/\sqrt{\tau/\mathrm{s}}$ for FO2-Cs and FO2-Rb and $3.2 \times 10^{-13}/\sqrt{\tau/\mathrm{s}}$ for IT-CsF2. For this measurement, the instability of IT-CsF2 was slightly higher than for the entire campaign.

For this analysis, we take as reference the secondary representation of the second for the Yb transition of 518 295 836 590 863.63 Hz, which has an uncertainty

TABLE I. Summary of the remote and local comparisons between INRIM and SYRTE. Here y is the fractional frequency deviation of the ratio (for Rb and Yb relative to the CCTF 2021 recommendations;); u is the total combined uncertainty; u_A is the statistical uncertainty of the measurement, derived from the measured instability and including the contribution from density shift uncertainty for FO2-Cs and FO2-Rb; and u_{B1} and u_{B2} are the systematic uncertainties of each standard. The last column reports the total measurement time.

	y ($\times 10^{-16}$)	u ($\times 10^{-16}$)	u_A ($\times 10^{-16}$)	u_{B1} ($\times 10^{-16}$)	u_{B2} ($\times 10^{-16}$)	Meas. time (d)
Remote comparisons						
FO2-Cs/IT-CsF2	−5.5	3.7	1.3	2.1	2.4	56.1
FO2-Rb/IT-CsF2	−1.5	3.8	1.3	2.5	2.4	60.1
IT-Yb1/FO2-Cs	−0.4	3.0	2.1	0.2	2.1	3.9
IT-Yb1/FO2-Rb	−4.2	3.2	1.9	0.2	2.5	4.0
Local comparisons						
FO2-Rb/FO2-Cs	3.7	3.5	0.6	2.5	2.1	99.7
IT-Yb1/IT-CsF2	−4.9	5.9	5.3	0.2	2.4	4.3

of 1.9×10^{-16}, as established by CCTF in 2021. The result for the comparison between IT-Yb1 and FO2-Cs is y(IT-Yb1/FO2-Cs) $= -0.4(3.0)\times10^{-16}$ with a statistical uncertainty of 2.1×10^{-16} for a total measurement time of 95 h, including the contribution from the zero-density extrapolation of FO2-Cs. Accordingly, the absolute frequency of Yb is 518 295 836 590 863.61(17) Hz. The result for IT-Yb1/FO2-Rb is y(IT-Yb1/FO2-Rb) $= -4.2(3.2)\times10^{-16}$ with a statistical uncertainty of 1.9×10^{-16} for a total measurement time of 95 h, including the contribution from the density extrapolation of FO2-Rb. The corresponding ratio between Yb and Rb frequencies is 75 833 197.545 114 168(24). The local comparison at INRIM between IT-Yb1 and IT-CsF2 in the same period results in an average of y(IT-Yb1/IT-CsF2) $= -4.9(5.9)\times10^{-16}$, corresponding to an absolute frequency of Yb of 518 295 836 590 863.38(31) Hz. The results are summarized in Table I. It should be noted that these measurements, as well as the measurements between fountains, are calculated only on the common uptime. Alternatively, it would be possible to extrapolate over dead time by using the H masers as flywheels [41,71,72] increasing the measurement time at the expense of an extra contribution of uncertainty. Our measurements are in good agreement with the recommendations of secondary representations of the second and previous measurements of the absolute frequency of Yb and Rb [9,41,69,73] and their ratios [74,75].

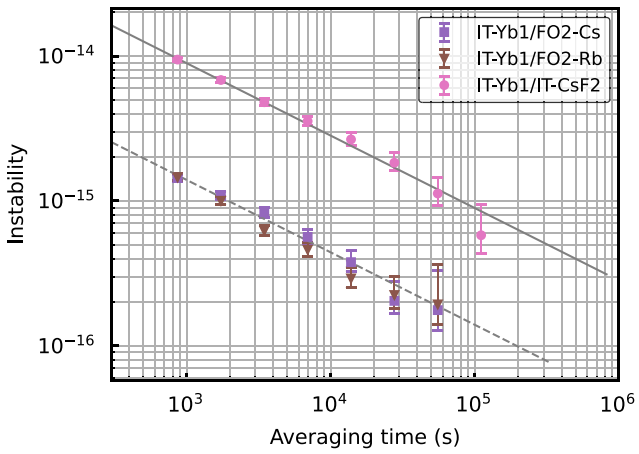

FIG. 5. Instabilities of the ratios between IT-Yb1 and FO2-Cs, FO2-Rb and IT-CsF2 as overlapping Allan deviation. The solid gray line represents the white noise contribution of IT-CsF2 (3.2×10^{-13} at 1 s for this shorter measurement); the dashed gray line represents the short-term instability of FO2-Rb and FO2-Cs (4.3×10^{-14} at 1 s).

IV. CONCLUSIONS AND PERSPECTIVES

We describe the operation and long-term characterization of the optical link between INRIM in Italy and SYRTE in France, which also represents a cross-border connection between the national facilities REFIMEVE and Italian Quantum Backbone. The present connection showed robust operation over the past four months and has been used to compare the Cs and Rb microwave frequency standards at the two Institutes, confirming their uncertainties at the 10^{-16} level. It allowed independent evaluations of the IT-Yb1/FO2-Cs and IT-Yb1/FO2-Rb ratios with uncertainties at the 3×10^{-16} level, limited by the microwave clocks. These measurements contribute to the milestones towards the redefinition of the second. Notably, the direct measurement of the Yb/Rb ratio performed in this work is consistent with the CCTF recommendation and improves the preceding measurement performed using data in the Circular T [74,75]. The link is planned to continue in the next years, with periodical comparison campaigns also involving other optical clocks at the two institutes, i.e., a Hg and Sr neutral lattice clocks at SYRTE [76,77], as well as a neutral lattice Sr clock under development at INRIM [78,79].

The interconnection between the infrastructures REFIMEVE and Italian Quantum Backbone demonstrates the integrability of national networks for frequency distribution at a European scale. Together with two other fiber links to NPL (UK) and PTB (Germany) [35], it opens the possibility of more composite clock comparison campaigns, including optical clocks based on different atomic species, neutral atoms, and ions, from four national metrology institutes. The richness of this network is an important resource for metrology and could support the computation of more accurate regional and global geodetic models [80–83] by providing centimeter-level precision estimates of the gravitational potential using optical clocks as probes [14,39,84], and the search for variations in fundamental constants and dark matter [21,22]. A prominent feature of this infrastructure is the optical continuity of the radiation between the two remote metrological institutes, which can be further exploited to investigate combined interrogation schemes of remote clocks [35] and support other research fields, such as long-distance quantum communication [85] and frequency distribution to telescope facilities [34]. The Italian Quantum Backbone reaches the Medicina radio telescope, which is part of the International Very Long Baseline Interferometry Network, the Matera Space Geodesy Centre and Satellite Laser Ranging facility, and the ground-based control station of Galileo, the European Global Navigation Satellite System. Beyond reaching the Laboratoire Souterrain de Modane in Modane, REFIMEVE is planned to connect the French Space Agency quarters in Toulouse, the lunar ranging and geodetic station of Observatoire de la Côte d'Azur, and the radiotelescopes of Observatoire de Paris-Nançay and Institut de Radioastronomie Millimétrique in the French Alps. The interconnection of such large facilities between them and to European Metrological Institutes is relevant to support Galileo itself and future European satellite missions such as ACES, and in perspective could stimulate a more extended exploitation of high-accuracy time-and-frequency references in geodesy, radio astronomy, and navigation.

ACKNOWLEDGMENTS

We acknowledge unfailing and continuing support from the network and engineering team of RENATER, and especially N. Quintin, X. Misseri, L. Gydé, and E. Camisard. We are grateful to Région Auvergne-Rhone-Alpes, Amplivia, Université Grenoble-Alpes (UGA) and Laboratoire Souterrain de Modane (LSM, UMR 6417 CNRS and UGA) and especially to O. Charrier (AMPLIVIA), R. Dorge, G. Enderlé (UGA), T. Zampieri (LSM), and J. Bernier (CNRS/IN2P3) for their great help in establishing the link Grenoble-Modane. We also thank Consortium TOPIX, especially M. Frittelli and A. Galardini, for access to the fibers on the Italian side. The Yb clock group is grateful to G. Cappellini, M. Takamoto, and H. Katori for assistance with the atomic source and to T. Legero for assistance with the optical cavity. The operation of the Yb clock is enabled by their help.

This work is supported by: the European Metrology Program for Innovation and Research (EMPIR) Projects 18SIB05 ROCIT, 18SIB06 TIFOON, 20FUN08 Next-Lasers, which received funding from the EMPIR programme cofinanced by the Participating States and from the European Union's Horizon 2020 research and innovation programme; the European Union's Horizon 2020 research and innovation programme under Grant Agreement No. 951886 (CLONETS-DS); Program "Investissements d'Avenir" launched by the French Government and implemented by Agence Nationale de la Recherche with references ANR-10-LABX-48-01 (Labex First-TF), ANR-21-ESRE-0029 (ESR/Equipex T-REFIMEVE), ANR-11-EQPX-0039 (Equipex REFIMEVE+), ANR-10-IDEX-0001-002 (Idex PSL); Conseil Régional Bourgogne-Franche-Comté; Domaine d'Intérêt Majeur Science et Ingénierie en Région Île-de-France pour les Technologies Quantiques (DIM SIRTEQ).

A.A.K., D.C., C.Ch., P.-E.P. coordinated the realization of the optical links in Italy and France, their interconnection, and coordinated this project. C.Cl., A.A.K., D.C., E.C., O.L., and P.-E.P. conceived and elaborated the architecture of the link. S.D., M.R., A.M., C.Cl. realized, characterized, and operated the optical-fiber link on the Italian side. M.R., M.P., and C.Cl. operated the INRIM comb and related frequency measurements. I.G., S.C., M.P. realized, characterized, and operated the Yb clock IT-Yb1. M.G., G.A.C., F.L. realized, characterized, and operated the Italian Cs fountain clock IT-CsF2. E.K.B. designed and realized the electronics used to operate the INRIM link and atomic clocks. E.C., O.L., M.T., M.M.L., and P.-E.P. realized, characterized, and operated the optical-fiber link on the French side. B.P. and R.L.T. operated the SYRTE comb and related frequency measurements. M.A. and L.L. realized, characterized, and operated the French Cs and Rb fountains and the oscillators required for their operation. M.L. and H.L.G. contributed to the operation and maintenance of the French Cs and Rb fountains during the comparison campaign. M.P. and C.Cl. analyzed the data produced and processed by the teams and wrote the paper, with relevant input and discussions with all the authors.

[1] A. Takamizawa, S. Yanagimachi, and K. Hagimoto, First uncertainty evaluation of the cesium fountain primary frequency standard NMIJ-F2, Metrologia **59**, 035004 (2022).

[2] S. Beattie, B. Jian, J. Alcock, M. Gertsvolf, R. Hendricks, K. Szymaniec, and K. Gibble, First accuracy evaluation of the NRC-FCs2 primary frequency standard, Metrologia **57**, 035010 (2020).

[3] S. Weyers, V. Gerginov, M. Kazda, J. Rahm, B. Lipphardt, G. Dobrev, and K. Gibble, Advances in the accuracy, stability, and reliability of the PTB primary fountain clocks, Metrologia **55**, 789 (2018).

[4] A. Jallageas, L. Devenoges, M. Petersen, J. Morel, L. G. Bernier, D. Schenker, P. Thomann, and T. Südmeyer, First uncertainty evaluation of the FoCS-2 primary frequency standard, Metrologia **55**, 366 (2018).

[5] J. Guéna, *et al.*, First international comparison of fountain primary frequency standards via a long distance optical fiber link, Metrologia **54**, 348 (2017).

[6] I. Y. Blinov, A. I. Boiko, Y. S. Domnin, V. P. Kostromin, O. V. Kupalova, and D. S. Kupalov, Budget of uncertainties in the cesium frequency frame of fountain type, Meas. Tech. **60**, 30 (2017).

[7] F. Fang, M. Li, P. Lin, W. Chen, N. Liu, Y. Lin, P. Wang, K. Liu, R. Suo, and T. Li, NIM5 Cs fountain clock and its evaluation, Metrologia **52**, 454 (2015).

[8] F. Levi, D. Calonico, C. E. Calosso, A. Godone, S. Micalizio, and G. A. Costanzo, Accuracy evaluation of ITCsF2: A nitrogen cooled caesium fountain, Metrologia **51**, 270 (2014).

[9] J. Guéna, M. Abgrall, A. Clairon, and S. Bize, Contributing to TAI with a secondary representation of the SI second, Metrologia **51**, 108 (2014).

[10] J. Guena, M. Abgrall, D. Rovera, P. Laurent, B. Chupin, M. Lours, G. Santarelli, P. Rosenbusch, M. E. Tobar, R. Li, K. Gibble, A. Clairon, and S. Bize, Progress in atomic fountains at LNE-SYRTE, IEEE Trans. Ultrason. Ferroelectr. Freq. Control **59**, 391 (2012).

[11] R. Li, K. Gibble, and K. Szymaniec, Improved accuracy of the NPL-CsF2 primary frequency standard: Evaluation of distributed cavity phase and microwave lensing frequency shifts, Metrologia **48**, 283 (2011).

[12] K. Beloy, *et al.*, Boulder Atomic Clock Optical Network (BACON) Collaboration, Frequency ratio measurements at 18-digit accuracy using an optical clock network, Nature **591**, 564 (2021).

[13] S. M. Brewer, J.-S. Chen, A. M. Hankin, E. R. Clements, C. W. Chou, D. J. Wineland, D. B. Hume, and D. R. Leibrandt, $^{27}Al^{+}$ Quantum-Logic Clock with a Systematic Uncertainty below 10^{-18}, Phys. Rev. Lett. **123**, 033201 (2019).

[14] W. F. McGrew, X. Zhang, R. J. Fasano, S. A. Schäffer, K. Beloy, D. Nicolodi, R. C. Brown, N. Hinkley, G. Milani, M. Schioppo, T. H. Yoon, and A. D. Ludlow, Atomic clock performance enabling geodesy below the centimetre level, Nature **564**, 87 (2018).

[15] I. Ushijima, M. Takamoto, M. Das, T. Ohkubo, and H. Katori, Cryogenic optical lattice clocks, Nat. Photonics **9**, 185 (2015).

[16] P. Gill, Is the time right for a redefinition of the second by optical atomic clocks?, J. Phys.: Conf. Ser. **723**, 012053 (2016).

[17] J. Lodewyck, On a definition of the SI second with a set of optical clock transitions, Metrologia **56**, 055009 (2019).

[18] F. Riehle, P. Gill, F. Arias, and L. Robertsson, The CIPM list of recommended frequency standard values: Guidelines and procedures, Metrologia **55**, 188 (2018).

[19] C. Sanner, N. Huntemann, R. Lange, C. Tamm, E. Peik, M. S. Safronova, and S. G. Porsev, Optical clock comparison for Lorentz symmetry testing, Nature **567**, 204 (2019).

[20] R. Lange, N. Huntemann, J. M. Rahm, C. Sanner, H. Shao, B. Lipphardt, C. Tamm, S. Weyers, and E. Peik, Improved Limits for Violations of Local Position Invariance from Atomic Clock Comparisons, Phys. Rev. Lett. **126**, 011102 (2021).

[21] B. M. Roberts, *et al.*, Search for transient variations of the fine structure constant and dark matter using fiber-linked optical atomic clocks, New J. Phys. **22**, 093010 (2020).

[22] P. Delva, *et al.*, Test of Special Relativity Using a Fiber Network of Optical Clocks, Phys. Rev. Lett. **118**, 221102 (2017).

[23] G. Panfilo and F. Arias, The coordinated universal time (UTC), Metrologia **56**, 042001 (2019).

[24] A. Bauch, J. Achkar, S. Bize, D. Calonico, R. Dach, R. Hlavać, L. Lorini, T. Parker, G. Petit, D. Piester, K. Szymaniec, and P. Uhrich, Comparison between frequency standards in Europe and the USA at the 10–15 uncertainty level, Metrologia **43**, 109 (2005).

[25] M. Pizzocaro, *et al.*, Intercontinental comparison of optical atomic clocks through very long baseline interferometry, Nat. Phys. **17**, 223 (2021).

[26] F. Riedel, *et al.*, Direct comparisons of European primary and secondary frequency standards via satellite techniques, Metrologia **57**, 045005 (2020).

[27] J. Leute, N. Huntemann, B. Lipphardt, C. Tamm, P. B. R. Nisbet-Jones, S. A. King, R. M. Godun, J. M. Jones, H. S. Margolis, P. B. Whibberley, A. Wallin, M. Merimaa, P. Gill, and E. Peik, Frequency comparison of $^{171}Yb^{+}$ ion optical clocks at PTB and NPL via GPS PPP, IEEE Trans. Ultrason. Ferroelectr. Freq. Control. **63**, 981 (2016).

[28] M. Fujieda, D. Piester, T. Gotoh, J. Becker, M. Aida, and A. Bauch, Carrier-phase two-way satellite frequency transfer over a very long baseline, Metrologia **51**, 253 (2014).

[29] H. Hachisu, M. Fujieda, S. Nagano, T. Gotoh, A. Nogami, T. Ido, S. Falke, N. Huntemann, C. Grebing, B. Lipphardt, C. Lisdat, and D. Piester, Direct comparison of optical lattice clocks with an intercontinental baseline of 9000 km, Opt. Lett. **39**, 4072 (2014).

[30] M. Musha, F.-L. Hong, K. Nakagawa, and K.-i. Ueda, Coherent optical frequency transfer over 50-km physical distance using a 120-km-long installed telecom fiber network, Opt. Express **16**, 16459 (2008).

[31] T. Akatsuka, T. Goh, H. Imai, K. Oguri, A. Ishizawa, I. Ushijima, N. Ohmae, M. Takamoto, H. Katori, T. Hashimoto, H. Gotoh, and T. Sogawa, Optical frequency distribution using laser repeater stations with planar lightwave circuits, Opt. Express **28**, 9186 (2020).

[32] C. Lisdat, *et al.*, A clock network for geodesy and fundamental science, Nat. Commun. **7**, 12443 (2016).

[33] S. Droste, F. Ozimek, T. Udem, K. Predehl, T. W. Hänsch, H. Schnatz, G. Grosche, and R. Holzwarth, Optical-Frequency Transfer over a Single-Span 1840 km Fiber Link, Phys. Rev. Lett. **111**, 110801 (2013).

[34] C. Clivati, R. Aiello, G. Bianco, C. Bortolotti, P. De Natale, V. Di Sarno, P. Maddaloni, G. Maccaferri, A. Mura, M. Negusini, F. Levi, F. Perini, R. Ricci, M. Roma, L. Santamaria Amato, M. Siciliani de Cumis, M. Stagni, A. Tuozzi,

and D. Calonico, Common-clock very long baseline interferometry using a coherent optical fiber link, Optica **7**, 1031 (2020).

[35] M. Schioppo, *et al.*, Comparing ultrastable lasers at 7×10^{-17} fractional frequency instability through a 2220 km optical fibre network, Nat. Commun. **13**, 212 (2022).

[36] D. Husmann, *et al.*, SI-traceable frequency dissemination at 1572.06 nm in a stabilized fiber network with ring topology, Opt. Express **29**, 24592 (2021).

[37] N. Chiodo, N. Quintin, F. Stefani, F. Wiotte, E. Camisard, C. Chardonnet, G. Santarelli, A. Amy-Klein, P.-E. Pottie, and O. Lopez, Cascaded optical fiber link using the internet network for remote clocks comparison, Opt. Express **23**, 33927 (2015).

[38] T. Takano, M. Takamoto, I. Ushijima, N. Ohmae, T. Akatsuka, A. Yamaguchi, Y. Kuroishi, H. Munekane, B. Miyahara, and H. Katori, Geopotential measurements with synchronously linked optical lattice clocks, Nat. Photonics **10**, 662 (2016).

[39] J. Grotti, *et al.*, Geodesy and metrology with a transportable optical clock, Nat. Phys. **14**, 437 (2018).

[40] A. Yamaguchi, M. Fujieda, M. Kumagai, H. Hachisu, S. Nagano, Y. Li, T. Ido, T. Takano, M. Takamoto, and H. Katori, Direct comparison of distant optical lattice clocks at the 10^{-16} uncertainty, Appl. Phys. Express **4**, 082203 (2011).

[41] M. Pizzocaro, F. Bregolin, P. Barbieri, B. Rauf, F. Levi, and D. Calonico, Absolute frequency measurement of the $^1S_0$—$^3P_0$ transition of ^{171}Yb with a link to international atomic time, Metrologia **57**, 035007 (2020).

[42] G. Petit, A. Kanj, S. Loyer, J. Delporte, F. Mercier, and F. Perosanz, 1×10^{-16} frequency transfer by GPS PPP with integer ambiguity resolution, Metrologia **52**, 301 (2015).

[43] G. Petit, Sub-10^{-16} accuracy GNSS frequency transfer with IPPP, GPS Solut. **25**, 22 (2021).

[44] V. Formichella, L. Galleani, G. Signorile, and I. Sesia, Robustness tests for an optical time scale, Metrologia **59**, 015002 (2022).

[45] J. Yao, J. A. Sherman, T. Fortier, H. Leopardi, T. Parker, W. McGrew, X. Zhang, D. Nicolodi, R. Fasano, S. Schäffer, K. Beloy, J. Savory, S. Romisch, C. Oates, S. Diddams, A. Ludlow, and J. Levine, Optical-Clock-Based Time Scale, Phys. Rev. Appl. **12**, 044069 (2019).

[46] W. R. Milner, J. M. Robinson, C. J. Kennedy, T. Bothwell, D. Kedar, D. G. Matei, T. Legero, U. Sterr, F. Riehle, H. Leopardi, T. M. Fortier, J. A. Sherman, J. Levine, J. Yao, J. Ye, and E. Oelker, Demonstration of a Timescale Based on a Stable Optical Carrier, Phys. Rev. Lett. **123**, 173201 (2019).

[47] H. Hachisu, F. Nakagawa, Y. Hanado, and T. Ido, Months-long real-time generation of a time scale based on an optical clock, Sci. Rep. **8**, 4243 (2018).

[48] D. Herman, S. Droste, E. Baumann, J. Roslund, D. Churin, A. Cingoz, J.-D. Deschênes, I. H. Khader, W. C. Swann, C. Nelson, N. R. Newbury, and I. Coddington, Femtosecond Timekeeping: Slip-Free Clockwork for Optical Timescales, Phys. Rev. Appl. **9**, 044002 (2018).

[49] F. Guillou-Camargo, V. Ménoret, E. Cantin, O. Lopez, N. Quintin, E. Camisard, V. Salmon, J.-M. Le Merdy, G. Santarelli, A. Amy-Klein, P.-E. Pottie, B. Desruelle, and C. Chardonnet, First industrial-grade coherent fiber link for optical frequency standard dissemination, Appl. Opt. **57**, 7203 (2018).

[50] https://www.refimeve.fr/index.php/en/.

[51] C. Clivati, G. Cappellini, L. F. Livi, F. Poggiali, M. S. de Cumis, M. Mancini, G. Pagano, M. Frittelli, A. Mura, G. A. Costanzo, F. Levi, D. Calonico, L. Fallani, J. Catani, and M. Inguscio, Measuring absolute frequencies beyond the GPS limit via long-haul optical frequency dissemination, Opt. Express **24**, 11865 (2016).

[52] B. Argence, B. Chanteau, O. Lopez, D. Nicolodi, M. Abgrall, C. Chardonnet, C. Daussy, B. Darquié, Y. Le Coq, and A. Amy-Klein, Quantum cascade laser frequency stabilization at the sub-Hz level, Nat. Photonics **9**, 456 (2015).

[53] O. Votava, S. Kassi, A. Campargue, and D. Romanini, Comb coherence-transfer and cavity ring-down saturation spectroscopy around 1.65 μm: kHz-accurate frequencies of transitions in the $2\nu3$ band of $^{12}CH_4$, Phys. Chem. Chem. Phys. **24**, 4157 (2022).

[54] K. Manamanni, T. Steshchenko, F. Wiotte, R. L. Targat, M. Abgrall, O. Lopez, E. Cantin, P. Éric Pottie, A. Amy-Klein, V. Roncin, and F. Du-Burck, Limitations due to residual interference in a fiber-based optical frequency reference at 1.55 μm, J. Opt. Soc. Am. B **39**, 438 (2022).

[55] C. Clivati, R. Ambrosini, T. Artz, A. Bertarini, C. Bortolotti, M. Frittelli, F. Levi, A. Mura, G. Maccaferri, M. Nanni, M. Negusini, F. Perini, M. Roma, M. Stagni, M. Zucco, and D. Calonico, A VLBI experiment using a remote atomic clock via a coherent fibre link, Sci. Rep. **7**, 40992 (2017).

[56] J. Serrano, P. Alvarez, M. Cattin, *et al.*, in *Int. Conf. Accelerator and Large Experimental Physics Control Systems (ICALEPCS), Kobe, Japan, 2009*, 978-4-9905391-0-8, TUC004 (CERN, Geneva, Switzerland, 2009).

[57] E. F. Dierikx, A. E. Wallin, T. Fordell, J. Myyry, P. Koponen, M. Merimaa, T. J. Pinkert, J. C. J. Koelemeij, H. Z. Peek, and R. Smets, White Rabbit precision time protocol on long-distance fiber links, IEEE Trans. Ultrason. Ferroelectr. Freq. Control **63**, 945 (2016).

[58] P. A. Williams, W. C. Swann, and N. R. Newbury, High-stability transfer of an optical frequency over long fiber-optic links, J. Opt. Soc. Am. B **25**, 1284 (2008).

[59] E. Cantin, M. Tønnes, R. Le Targat, A. Amy-Klein, O. Lopez, and P.-E. Pottie, An accurate and robust metrological network for coherent optical frequency dissemination, New J. Phys. **23**, 053027 (2021).

[60] C. E. Calosso, E. K. Bertacco, D. Calonico, C. Clivati, G. A. Costanzo, M. Frittelli, F. Levi, S. Micalizio, A. Mura, and A. Godone, Doppler-stabilized fiber link with 6 dB noise improvement below the classical limit, Opt. Lett. **40**, 131 (2015).

[61] A. Bercy, F. Stefani, O. Lopez, C. Chardonnet, P.-E. Pottie, and A. Amy-Klein, Two-way optical frequency comparisons at 5×10^{-21} relative stability over 100-km telecommunication network fibers, Phys. Rev. A **90**, 061802(R) (2014).

[62] D. Xu, O. Lopez, A. Amy-Klein, and P.-E. Pottie, Nonreciprocity in optical fiber links: Experimental evidence, Opt. Express **29**, 17476 (2021).

[63] S. Koke, A. Kuhl, T. Waterholter, S. M. F. Raupach, O. Lopez, E. Cantin, N. Quintin, A. Amy-Klein, P.-E. Pottie, and G. Grosche, Combining fiber Brillouin amplification with a repeater laser station for fiber-based optical frequency dissemination over 1400 km, New J. Phys. **21**, 123017 (2019).

[64] C. Clivati, M. Frittelli, D. Calonico, A. Mura, and F. Levi, in *2015 Joint Conference of the IEEE International Frequency Control Symposium & the European Frequency and Time Forum* (IEEE, 2015), p. 579.

[65] Consultative Committee for Time and Frequency (CCTF), Recommendation CCTF PSFS 2: Updates to the CIPM list of standard frequencies (2021).

[66] K. Szymaniec and S. E. Park, Primary frequency standard NPL-CsF2: Optimized operation near the collisional shift cancellation point, IEEE Trans. Instrum. Meas. **60**, 2475 (2015).

[67] J. Lodewyck, R. Le Targat, P.-E. Pottie, E. Benkler, S. Koke, and J. Kronjäger, Universal formalism for data sharing and processing in clock comparison networks, Phys. Rev. Res. **2**, 043269 (2020).

[68] https://www.bipm.org/en/bipm/tai/.

[69] M. Pizzocaro, P. Thoumany, B. Rauf, F. Bregolin, G. Milani, C. Clivati, G. A. Costanzo, F. Levi, and D. Calonico, Absolute frequency measurement of the $^1S_0$—$^3P_0$ transition of ^{171}Yb, Metrologia **54**, 102 (2017).

[70] H. R. Telle, B. Lipphardt, and J. Stenger, Kerr-lens, mode-locked lasers as transfer oscillators for optical frequency measurements, Appl. Phys. B **74**, 1 (2002).

[71] C. Grebing, A. Al-Masoudi, S. Dörscher, S. Häfner, V. Gerginov, S. Weyers, B. Lipphardt, F. Riehle, U. Sterr, and C. Lisdat, Realization of a timescale with an accurate optical lattice clock, Optica **3**, 563 (2016).

[72] N. Nemitz, T. Gotoh, F. Nakagawa, H. Ito, Y. Hanado, T. Ido, and H. Hachisu, Absolute frequency of ^{87}Sr at 1.8×10^{-16} uncertainty by reference to remote primary frequency standards, Metrologia **58**, 025006 (2021).

[73] H. Kim, M.-S. Heo, C. Y. Park, D.-H. Yu, and W.-K. Lee, Absolute frequency measurement of the ^{171}Yb optical lattice clock at KRISS using TAI for over a year, Metrologia **58**, 055007 (2021).

[74] W. F. McGrew, X. Zhang, H. Leopardi, R. J. Fasano, D. Nicolodi, K. Beloy, J. Yao, J. A. Sherman, S. A. Schäffer, J. Savory, R. C. Brown, S. Römisch, C. W. Oates, T. E. Parker, T. M. Fortier, and A. D. Ludlow, Towards the optical second: Verifying optical clocks at the SI limit, Optica **6**, 448 (2019).

[75] T. Kobayashi, D. Akamatsu, K. Hosaka, Y. Hisai, M. Wada, H. Inaba, T. Suzuyama, F.-L. Hong, and M. Yasuda, Demonstration of the nearly continuous operation of an ^{171}Yb optical lattice clock for half a year, Metrologia **57**, 065021 (2020).

[76] R. Tyumenev, M. Favier, S. Bilicki, E. Bookjans, R. L. Targat, J. Lodewyck, D. Nicolodi, Y. L. Coq, M. Abgrall, J. Guéna, L. D. Sarlo, and S. Bize, Comparing a mercury optical lattice clock with microwave and optical frequency standards, New J. Phys. **18**, 113002 (2016).

[77] J. Lodewyck, S. Bilicki, E. Bookjans, J.-L. Robyr, C. Shi, G. Vallet, R. L. Targat, D. Nicolodi, Y. L. Coq, J. Guéna, M. Abgrall, P. Rosenbusch, and S. Bize, Optical to microwave clock frequency ratios with a nearly continuous strontium optical lattice clock, Metrologia **53**, 1123 (2016).

[78] M. Barbiero, M. G. Tarallo, D. Calonico, F. Levi, G. Lamporesi, and G. Ferrari, Sideband-Enhanced Cold Atomic Source for Optical Clocks, Phys. Rev. Appl. **13**, 014013 (2020).

[79] M. Barbiero, D. Calonico, F. Levi, and M. G. Tarallo, Optically loaded strontium lattice clock with a single multi-wavelength reference cavity, IEEE Trans. Instrum. Meas. **71**, 1 (2022).

[80] R. Bondarescu, M. Bondarescu, G. Hetényi, L. Boschi, P. Jetzer, and J. Balakrishna, Geophysical applicability of atomic clocks: Direct continental geoid mapping, Geophys. J. Int. **191**, 78 (2012).

[81] R. Bondarescu, A. Schärer, A. Lundgren, G. Hetényi, N. Houlié, P. Jetzer, and M. Bondarescu, Ground-based optical atomic clocks as a tool to monitor vertical surface motion, Geophys. J. Int. **202**, 1770 (2015).

[82] G. Lion, I. Panet, P. Wolf, C. Guerlin, S. Bize, and P. Delva, Determination of a high spatial resolution geopotential model using atomic clock comparisons, J. Geod. **91**, 597 (2017).

[83] T. E. Mehlstäubler, G. Grosche, C. Lisdat, P. O. Schmidt, and H. Denker, Atomic clocks for geodesy, Rep. Progr. Phys. **81**, 064401 (2018).

[84] M. Takamoto, I. Ushijima, N. Ohmae, T. Yahagi, K. Kokado, H. Shinkai, and H. Katori, Test of general relativity by a pair of transportable optical lattice clocks, Nat. Photonics **14**, 411 (2020).

[85] C. Clivati, A. Meda, S. Donadello, S. Virzö, M. Genovese, F. Levi, A. Mura, M. Pittaluga, Z. Yuan, A. J. Shields, M. Lucamarini, I. P. Degiovanni, and D. Calonico, Coherent phase transfer for real-world twin-field quantum key distribution, Nat. Commun. **13**, 157 (2022).